Pergamon

Cement and Concrete Research, Vol. 26, No. 9, pp. 1409-1422, 1996

0008-8846/96 $15.00 + .00

PII S0008-8846(96)00114-7

TRANSIENT CREEP OF CONCRETE UNDER BIAXIAL STRESS AND HIGH TEMPERATURE

K.-Ch. Thienel and F.S. Rostásy
Institut für Baustoffe, Massivbau und Brandschutz der Technischen Universität
Braunschweig, Beethovenstr. 52, 38106 Braunschweig, Germany

(Refereed)
(Received April 13, 1995; in final form June 13, 1996)

ABSTRACT

Understanding concrete behavior under transient high temperature is an important aspect of structural fire research. Consequently, many investigations have been performed under uniaxial loading conditions, but, only a few under biaxial states of stress. This report has two primary goals. The mechanical behavior of unsealed concrete and mortar was studied under biaxial stresses and transient temperature. Furthermore, the influence of the concrete composition was investigated for quartzitic concrete and mortar in thermal expansion tests and biaxial transient creep tests. Based on the test results a model of the transient creep of concrete under multiaxial loading is proposed. In combination with a suitable high temperature failure model, this model is applicable for concretes with different compositions.

Introduction

The behavior of structural elements exposed to high temperature has usually been examined in uniaxial transient creep tests, e.g. [1, 2, 3, 4]. Different influences were examined in these studies: the type of aggregate, the curing conditions and the stress level α ($\alpha = \sigma_{1,20} : f_{1,20}$). The first tests of symmetrical biaxial transient creep of concrete [5] indicated that transient creep under biaxial loading differs from that under uniaxial loading; however, no clear dependency could be stated.

The type of aggregate affects the transient creep strains significantly above 450°C, especially if quartzitic aggregate is used. In addition, transient creep strains depend on the type of cement used in the temperature range above 200°C [6]. The results also show the significance of the Al_2O_3 content of the cement used above 400°C [7]. A more detailed description of the latter effect is needed.

Concrete composition significantly influences the transient creep of concrete. This is obvious because transient creep only occurs in the cement paste [2]. A disadvantage of recent investigations is the simultaneous variation of the aggregate/cement ratio and of the water/cement ratio. Therefore the individual influence of both parameters is still not clear.

The stress state is an important influence as well. Most investigations are based on uniaxial tests performed at different stress levels α ($\alpha = \sigma_{1,20} : f_{1,20}$). Only a few results are available regarding the influence of the stress ratio κ ($\kappa = \sigma_{2,20} : \sigma_{1,20}$) [5]. These results are

inconsistent and restricted to symmetrical biaxial stresses. Thus it was the goal of the investigation to improve the knowledge in this field.

Materials and Methods

Specimens, Materials and Test Procedure. The tests were performed with panels (200 · 200 ·50 mm³). These panels were saw-cut from cubes after at least 90 days. The standard curing regime for all specimens was: demoulding after 1 day with subsequent underwater curing for 7 days, followed by storage at 20°C/65 % r.h.

Three concretes and one mortar with the same quartzitic aggregate were tested. The concretes differ with respect to the aggregate/cement ratio, A/C, and the water/cement ratio, W/C. The mortar differs from the concretes with respect to the maximum aggregate size, d_{max}, and the aggregate/cement ratio. The cement used in this investigation was German Portland cement CEM I 32,5R. Detailed compositions are given in Table 1.

All specimens were loaded at ambient temperature to a stress level of $\alpha(\kappa) = 0.0, 0.15, 0.30$ and 0.45 respective to the corresponding ultimate strength $f_{1,20}(\kappa)$ at room temperature and the same stress ratio $\kappa = \sigma_{2,20} : \sigma_{1,20}$. This method ensured the same stress level for uniaxial and biaxial loading. The tests described in this paper were performed at stress ratios $\kappa = 0.0$, 0.4 and 0.7. The unsealed specimens were heated at a constant rate of 2 K/min. During the transient creep tests the stress level α and the stress ratio κ were kept constant and the resulting strains were measured; the results for the three concretes will be discussed in detail.

Test Setup. The tests were performed in a special biaxial high temperature testing frame described in detail in [5, 7]. A brief outline will be given here. The loading system consists of a closed rigid steel frame. Loading is applied by a closed-loop system comprising four servohydraulic jacks with a maximum load of 1000 kN in compression and 270 kN in tension. The compressive forces were transmitted by water-cooled heat-resistant pistons. Compressive load was applied by brushes to provide for a homogeneous stress state [9]. Position of the specimen in the center of load was ensured by a master-slave control technology between the opposite hydraulic jacks. Deformations were measured in all axes by means of LVDTs. The latter were mounted on special high-temperature dilatometers [5].

The specimen was heated via its free surfaces by a controlled electrical furnace, with a maximum temperature is 1000°C. A removable furnace enclosed the specimen and parts of

TABLE 1

Concrete Composition

Type of Concrete	$f_{1,20}$ [MPa]	Cement Content, C [kg/m³]	Mix Proportions by Weight (C:A:W)	d_{max} [mm]	Plasticizer (% of Cement Content)	Air [%]
QB1	35.5	292	1:6.84:0.45	16	3	1.9
QB2	45.0	346	1:5.45:0.45	16	-	2.1
QB3	35.6	328	1:5.47:0.61	16	-	1.8
M	35.0	562	1:3.00:0.48	2	-	5.9

the loading system. Three separate adjustable heating circuits ensured a homogeneous temperature distribution. Temperature was controlled by four thermocouples placed on the specimen surface.

Results and Discussion

Thermal Strain. Variations in the aggregate/cement ratio significantly influence the thermal expansion of concrete and mortar (Fig. 1). The thermal strains of the concretes and mortar are depicted at selected temperature levels with the aggregate/cement ratio as the parameter on the horizontal axis. Up to 150°C the influence of the aggregate content is rather small. It becomes more pronounced as temperature increases. The water/cement ratio had only a slight influence on the thermal strain. The observed differences are within the range of the experimental scatter.

Transient Creep. Discussion and analysis of the results of the transient creep tests are performed in terms of the transient octahedral creep strains ε_{0tr} and γ_{0tr}. The transient creep strains in the principle axes are expressed by Eq. 1 on the basis of the measured strains:

$$\varepsilon_{itr}(\sigma, T) = \varepsilon_{i,tot}(\sigma, T) - \varepsilon_{th}(T) - \varepsilon_{i,el,20}(\sigma) \ , \qquad (1)$$

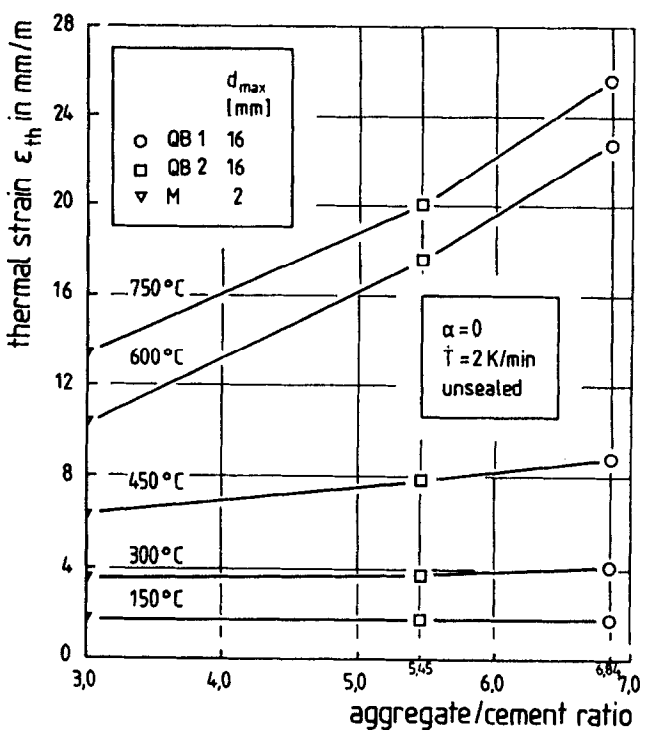

FIG. 1.
Influence of aggregate content on thermal strain of concrete.

where: $\varepsilon_{itr}(\sigma, T)$ = transient creep strain; $\varepsilon_{i,tot}(\sigma, T)$ = total strain; $\varepsilon_{th}(T)$ = thermal expansion; and $\varepsilon_{i,el,20}(\sigma)$ = elastic strain at ambient temperature, and i = 1, 2, 3.

The transient hydrostatic creep strain ε_{0tr} and the transient deviatoric creep strain γ_{0tr} can then be calculated using Eqs. 2 and 3:

$$\varepsilon_{0tr} = \frac{\varepsilon_{1tr} + \varepsilon_{2tr} + \varepsilon_{3tr}}{3}, \tag{2}$$

$$\gamma_{0tr} = \frac{2}{3}\sqrt{\left(\varepsilon_{1tr} - \varepsilon_{2tr}\right)^2 + \left(\varepsilon_{2tr} - \varepsilon_{3tr}\right)^2 + \left(\varepsilon_{3tr} - \varepsilon_{1tr}\right)^2} \tag{3}$$

Fig. 2 shows in the upper part the temperature dependent development of the transient octahedral creep strains. The deviatoric transient creep strains γ_{0tr} increase continuously with

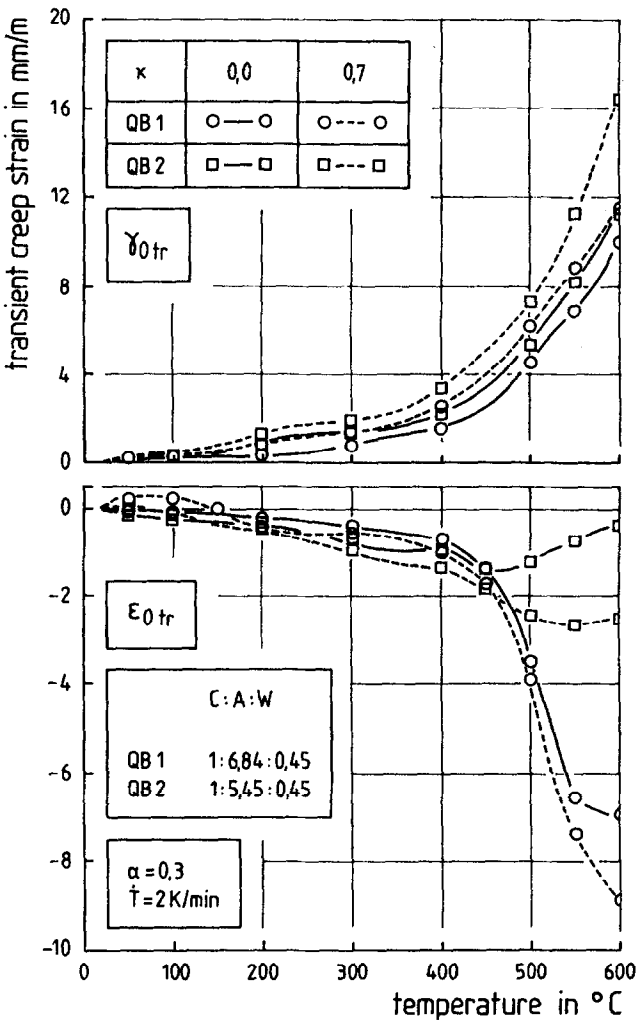

FIG. 2.
Influence of the aggregate content on transient octahedral creep strains.

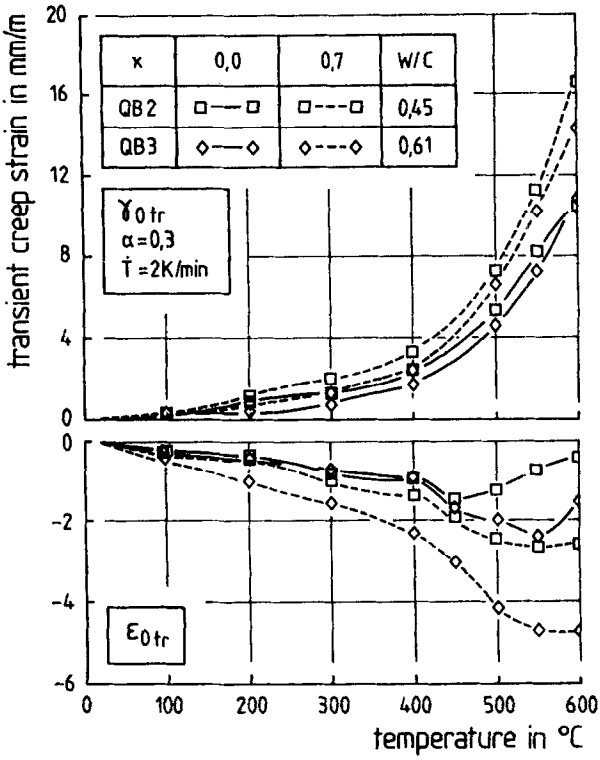

FIG. 3.
Influence of the water/cement ratio on transient octahedral creep strain.

temperature. Simultaneously the difference between the transient creep strain curves due to the variation in the aggregate content increases. The lower aggregate/cement ratio causes higher transient creep strains γ_{0tr} irrespective of the stress ratio κ.

A different behavior is obvious in the case of the hydrostatic transient creep strain ε_{0tr} (bottom part of Fig. 2). Soon after the onset of heating a more or less pronounced expansion occurs under biaxial loading. This behavior was also observed for other concretes [7]. It can be attributed to the moisture content of the specimens. High hydrostatic stresses under biaxial loading close shrinkage cracks, thus hampering evaporation. The consequence is a higher moisture content in a stressed specimen compared with an unstressed specimens in thermal expansion tests. The observed expansion during the transient creep tests in the temperature range from 50°C to 100°C must therefore be attributed to the thermal expansion of the higher residual water content.

For temperatures up to 450°C the leaner concrete exhibits smaller transient hydrostatic creep strains ε_{0tr} compared to the concrete with a higher aggregate content (Fig. 2). Transient hydrostatic creep strains of the uniaxially stressed specimen are smaller than those of the biaxially stressed specimens. The differences which result from the stress ratio κ remain stable until the end of the tests at 600°C. On the other hand the influence of the aggregate/cement ratio is reversed at about 450°C, due to the disintegration of the Portlandite in the temperature range 450°C to 550°C. While for the leaner concrete the compression increases extremely, the richer concrete already has reached a maximum in compression. For

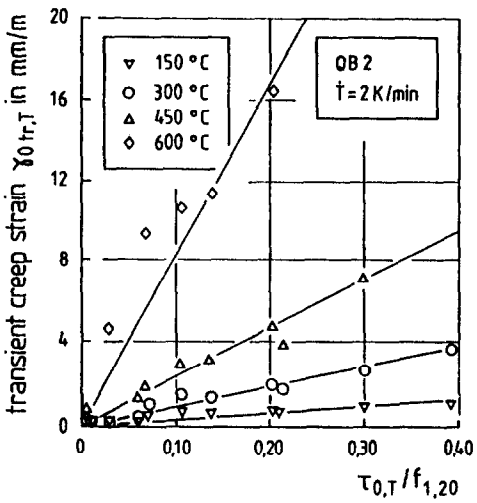

FIG. 4.
Stress dependence of the transient deviatoric creep strains at different temperatures.

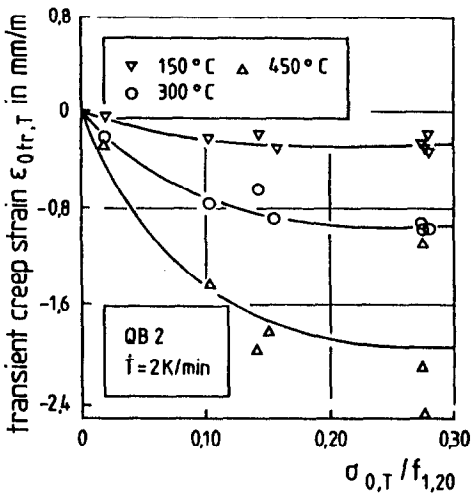

FIG. 5.
Stress dependence of the transient hydrostatic creep strains at different temperatures.

the leaner mix a maximum is also expected at higher temperatures, because these curves already exhibit a reversing point above 500°C.

Variations in the water/cement ratio affect both transient octahedral creep strains. In the upper part of Fig. 3 all transient deviatoric creep curves, γ_{0tr} , show, that a higher water/cement ratio has almost the same effect as a higher aggregate/cement ratio (see Fig. 2). The influence of the stress ratio κ is less pronounced.

The lower part of Fig. 3 shows the corresponding transient hydrostatic creep strains ε_{0tr}. A higher water/cement ratio results in a higher transient hydrostatic creep strain. The differences in the creep strains increase with increasing temperature - especially above 450°C. The effect of a higher water/cement ratio again is similar to the influence of a higher aggregate content, even though the resulting differences between the transient hydrostatic creep strain curves are smaller.

Both foregoing figures have shown the influence of the stress ratio κ on the transient octahedral creep strains γ_{0tr} and ε_{0tr}. It is well known that the magnitude of transient creep strain depends on the stress level α. The influence of both, the stress ratio κ and the stress level α, can easily be taken into account if the loading is expressed in terms of the octahedral stresses σ_0 and τ_0 instead of the principle stresses σ_1 and σ_2. The octahedral stresses can be determined from the applied stresses σ_1 and σ_2 by Eqs. (4) and (5):

$$\sigma_0 = \frac{\sigma_1 + \sigma_2 + \sigma_3}{3}, \tag{4}$$

$$\tau_0 = \frac{2}{3}\sqrt{(\sigma_1 - \sigma_2)^2 + (\sigma_2 - \sigma_3)^2 + (\sigma_3 - \sigma_1)^2} \tag{5}$$

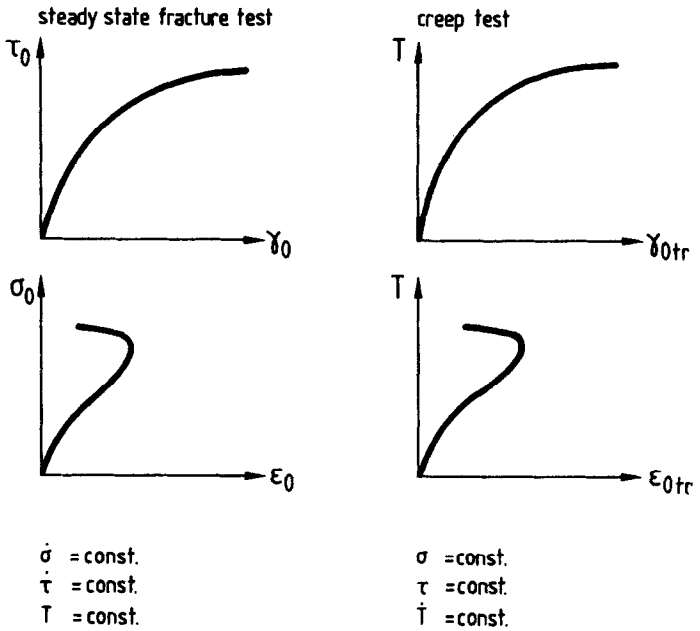

FIG. 6.
Schematic description of the similarity between the strains measured during steady state fracture test and transient creep test

Fig. 4 shows the dependence of the transient deviatoric creep strain γ_{0tr} on τ_0 at four different temperature levels. The octahedral shear stress τ_0 is normalized with respect to the uniaxial strength $f_{1,20}$ at normal temperature. A linear relationship between γ_{0tr} and τ_0 is obvious throughout the whole temperature range. The relationship between ε_{0tr} and σ_0 is nonlinear as is shown in Fig. 5. After an initial increase the transient hydrostatic creep strains seem to reach a maximum in compression at a stress level $\sigma_{0,T} / f_{1,20} = 0.30$.

The load dependence can be explained on basis of the structural alterations which occur in a stressed specimen during heat-up. Rostásy et al. [10] stated, that the original distribution of the mechanical stresses in the matrix changes during heat-up due to transient creep of the cement paste. This stress redistribution influences the thermally induced development of cracks, irrespective of the applied stress ratio κ. Differences result only from the applied stress level α. These structural alterations of the concrete matrix due to the external stresses are reflected particularly in the development of the transient hydrostatic creep strains ε_{0tr} with increasing hydrostatic stress σ_0. The observed behavior can be explained as follows. At first, lower hydrostatic stresses close the thermally induced cracks or at least suppress the development of cracks. A further increase of the hydrostatic stresses then compresses the concrete. To achieve the same strain differences in the latter case higher differences in the hydrostatic stresses are necessary. Supposing a continuous transition between these processes, then a good agreement with the experimental observations becomes obvious. The assumed separation of the above mentioned processes is supported by results obtained by means of acoustic emission analysis [11].

Modeling

Mathematical descriptions of the axial transient creep strain ε_{1tr} under uniaxial stress have already been published [1, 3]. These models are able to describe the transient creep strains of multiaxially stressed concrete, if assumptions are made regarding the development of Poisson's ratio [12] or if the transient creep functions are given in terms of the octahedral values. A more sophisticated model based on octahedral strains was published in [13]. Here a new way to describe the transient creep is proposed. The transient creep strain will be described by modified formulations, which are originally used for multiaxial stress-strain curves measured at normal temperature. Fig. 6 gives an outline of the underlying analogy in terms of octahedral strains and stresses. In the left part of Fig. 6 both octahedral strains ε_0 and γ_0 are given on the horizontal axes, while the corresponding octahedral stresses σ_0 and τ_0 are given on the vertical axes; temperature is a constant. In the right part of Fig. 6 a combined thermo-mechanical loading replaces the mechanical stresses in the left part of the figure. The transient octahedral strains ε_{0tr} and γ_{0tr} are now given on the horizontal axes, while the corresponding thermo-mechanical loading is represented by the temperature T is on the vertical axes, the octahedral stresses σ_0 and τ_0 are constants.

In [7, 8] the applicability of the incremental formulation of the deformation behavior at normal temperature of Stankowski and Gerstle [14] to describe the behavior of multiaxially stressed concrete at high temperature was demonstrated. This model is an incremental formulation based on the octahedral bulk modulus K, the octahedral shear modulus G and two coupling moduli H and Y. Its analytical formulation is given in [14, 15, 16]. This model will now be used for transient creep. Only the necessary modifications are explained here.

The stresses can be calculated by the temperature dependent failure model presented in [8]. The increments of the transient octahedral creep strains are given by Eq. (6):

$$\begin{Bmatrix} \Delta\varepsilon_{0tr} \\ \Delta\gamma_{0tr} \end{Bmatrix} = \begin{bmatrix} \frac{1}{3K_{tr}} & \frac{1}{H_{tr}} \\ \frac{1}{Y_{tr}} & \frac{1}{2G_{tr}} \end{bmatrix} \cdot \begin{Bmatrix} \sigma_0 \cdot \frac{\Delta T}{T_0} \\ \tau_0 \cdot \frac{\Delta T}{T_0} \end{Bmatrix}. \tag{6}$$

The moduli in Eq. (6) will be referred to as "transient moduli". They replace the usually used moduli. The transient moduli have been determined on basis of results from transient creep tests like those shown in Figs. 2 and 3. The transient bulk modulus K_{tr} decreases linearly with increasing temperature. This assumption is only a crude approximation of the real behavior, but it was maintained for the sake of simplicity [15]:

$$K_{tr} = K_{0tr}\left[1 - C_{kt}\frac{T}{T_0}\right], \tag{7}$$

$C_{kt} = 0.02$ [-] .

The transient bulk modulus K_{tr} depends significantly on the stress level $\alpha_\sigma = \sigma_0/f_1$ (see Fig. 5). This influence is taken into account by substituting K_{0tr} given by Eq. (8) into Eq. (7):

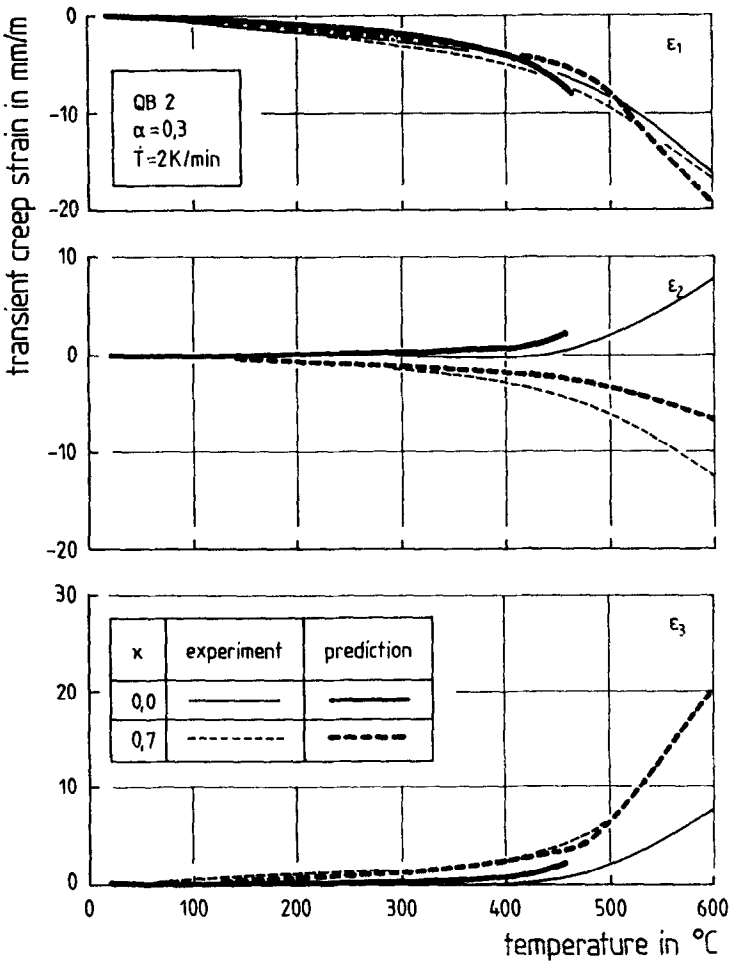

FIG. 7.
Comparison of measured and calculated transient creep strains for different stress ratios κ.

$$K_{0tr} = K_{0,20}\left(1 + C_{k,tr} \cdot \sigma_0\right) \cdot \left[\frac{\tau_0}{C_{k,\tau}}\right]^{\frac{3}{2}}, \tag{8}$$

with values of $C_{k,tr} = 0.25$ [MPa^{-1}] and $C_{k,\tau} = 45$ [MPa].

The transient shear modulus G_{tr} depends on stress level and temperature in a similar way. It decreases linearly from the initial value for $\tau_0 = 0$ to a value of zero for $\tau_0 = \tau_{0u,T}$, the temperature dependent shear strength, respectively, to a value of zero for $T = T_{crit}$, the critical temperature. Similar equations describe both, $\tau_{0u,T}$ and T_{crit}. The shear strength $\tau_{0u,T}$ is defined as the intersection of the actual stress vector with the temperature dependent failure surface given in [8]. $\tau_{0u,T}$ must be calculated for each temperature increment. The critical temperature can be determined in a similar way. T_{crit} was defined in [3, 7] as that temperature, at which a specimen under a constant stress level α fails during heat-up. With this

definition in mind, the critical temperature T_{crit} can be derived from the temperature dependent failure surface. Test results in [7] exhibit for all concretes an upper limit for the increase of the transient deviatoric creep strain. Therefore the decrease of G_{tr} is limited by Eq. (10).

$$G'_{0tr} = G_{0tr} \cdot C_{gt} \cdot \left[1 - \frac{T}{T_{crit}}\right] \quad \text{and} \tag{9}$$

$$G_{tr} = G'_{0tr} \cdot \left[1 - \frac{\tau_0}{\tau_{0u,t}}\right] \geq C_{g,tr} \cdot G, \tag{10}$$

with $C_{g,tr} = 0.2$ [-]. The initial value of the transient shear modulus G_{0tr} remains a function of the hydrostatic stress σ_0 as in the basic model [14]:

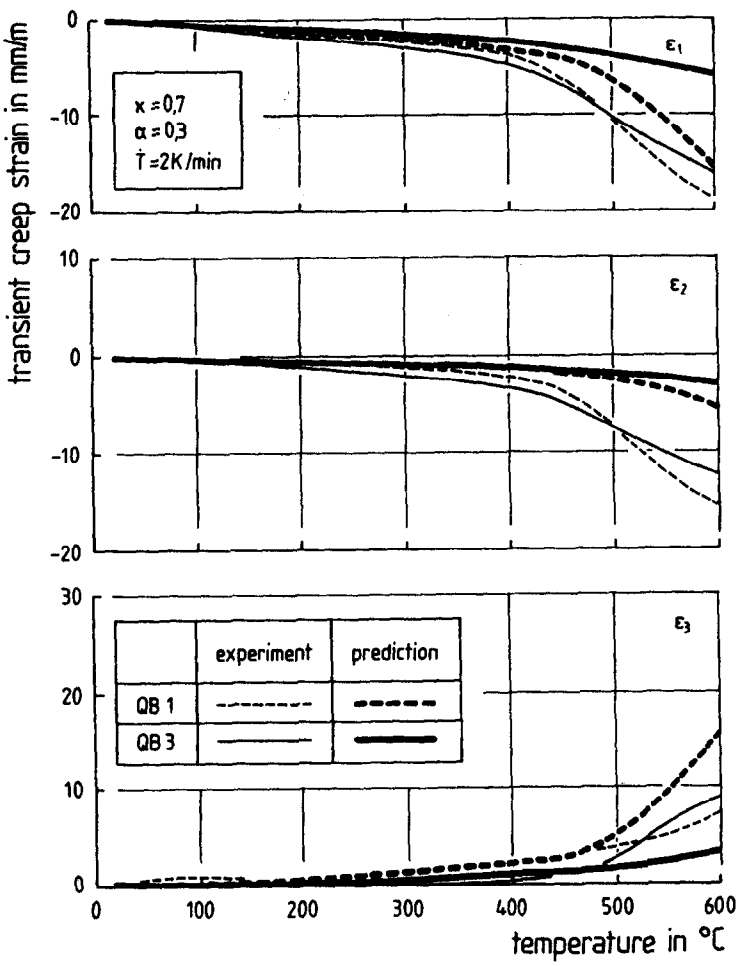

FIG. 8.
Comparison of measured and calculated transient creep strains for different concretes.

TABLE 2

Initial Bulk and Shear Moduli

Type of Concrete	$K_{0,20}$ [GPa]	$G_{0,20}$ [GPa]
QB1	27.39	16.11
QB2	19.32	16.92
QB3	24.68	16.52

$$G_{0tr} = G_{0,20} \cdot \left[1 - C_g \cdot \sigma_0\right] \geq C_g' \cdot G_{0,20} \quad , \tag{11}$$

with $C_g = 0.021$ [MPa^{-1}] and $C_g' = 0.47\left[-\right]$. The coupling moduli H_{tr} and Y_{tr} in Eq. (6) are given by Eqs. (12) and (13) according to the definition in [14]. Both coupling moduli depend on the combined thermo-mechanical loading:

$$H_{tr} = 50 + \frac{250}{\sigma_0\left[\frac{T}{T_0} - 20\right]} \quad , \quad \frac{T}{T_0} \geq 20\left[-\right], \tag{12}$$

$$Y_{tr} = \left[\frac{20 \cdot T_0}{\tau_0 \cdot T}\right]^2 . \tag{13}$$

Fig. 7 depicts for each principle axis separately the uniaxial and biaxial transient creep strains for concrete QB2 under a stress ratio $\kappa = 0.7$. Fig. 8 gives a comparison of measured and predicted transient creep strains for the two other concretes used. The agreement between the measured and the predicted transient creep strains is good. Deviations from the measured curves can be observed above 500°C. The initial values of the bulk modulus $K_{0,20}$ and the shear modulus $G_{0,20}$ which were used for the comparisons in Figs. 7, 8, and 9 were determined from steady state fracture tests [7] and are given in Table 2.

The proposed model is also able to predict the development of restraint. Fig. 9 shows a comparison between predicted restraint stresses for concrete QB2 and actual measurements taken from [17]. The agreement is reasonable up to 200°C. Beyond this temperature the measured restraint approaches the temperature dependent compressive strength of unloaded heated concrete specimen [7]. Because the underlying high temperature failure model is based on tests with concrete specimens, which were unloaded during heat-up, the failure model is unable to predict the strengthening effect due to the loading during heat-up. This disadvantage leads to an underestimation of the effective concrete strength. The consequence is a significant decrease in the transient modulus G_{tr} (see Eqs. (9) and (10)) which prevents an increase of the predicted restraint above 250°C.

Conclusions

It was the scope of the research project presented here to investigate transient creep of concrete at high temperature under biaxial stresses and to model the behavior accordingly. Be-

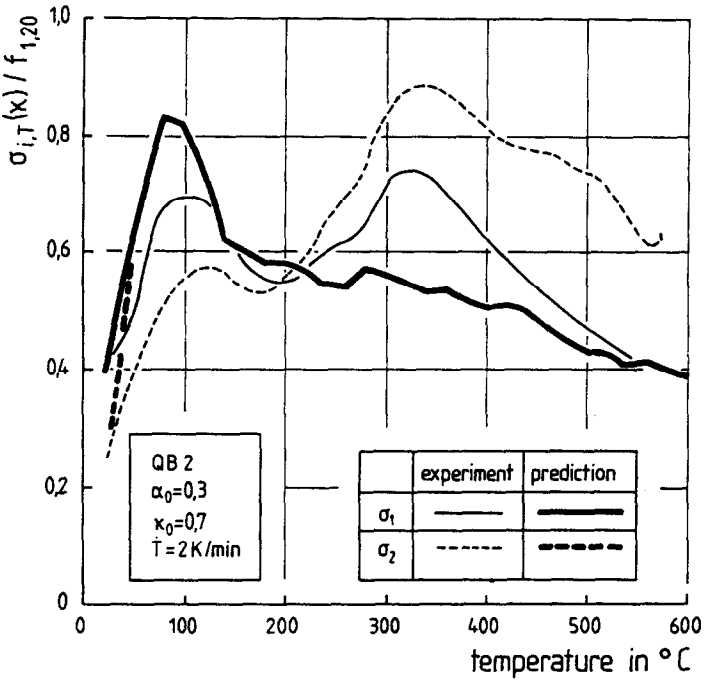

FIG. 9.
Comparison of measured and calculated restraint stresses.

sides, the influence of concrete composition should be studied. Test results were obtained for three quartzitic concretes and one mortar, having different aggregate/cement ratios, water/cement ratios and maximum aggregate sizes.

The composition of concrete influences the transient creep strains. Hereby the aggregate/cement ratio and the water/cement ratio are parameters of roughly the same influence. Alterations in the temperature dependent behavior of concrete due to the different concrete composition become more pronounced in the course of the decomposition of the Portlandite which occurs in the temperature range of 450°C to 550°C.

Using the octahedral expression for stresses and transient creep strains allows treating the influence of different stress ratios κ and different stress levels α in a similar way. Thus, both can be expressed by only using the stress levels α of the octahedral stresses as parameter. Using octahedral expressions permits tracing back differences in the transient creep which result from different stress ratios κ to differences in the stress level α of the octahedral stresses.

A new way to describe the transient creep strains is proposed. Based on the observed analogy in the development of the octahedral strain in transient creep tests and steady state fracture tests, transient creep is regarded as strains caused by thermo-mechanical loading. The deformation model of Stankowski and Gerstle is adopted and modified to describe transient creep. The applicability of the model is demonstrated for quartzitic concretes of different composition.

References

1. Anderberg, Y.; Thelandersson, S.: Stress and deformation characteristics of concrete at high temperatures, 2. Experimental investigation and material behavior model. Bulletin 54, Lund Institute of Technology, 1976.
2. Khoury, G.A.: Transient thermal creep of nuclear reactor pressure vessel type concrete. Vol. 1-3, Ph.D. Thesis University of London, 1983.
3. Schneider, U.: Ein Beitrag zur Frage des Kriechens und der Relaxation von Beton unter hohen Temperaturen. Habilitation Technical University Braunschweig, 1979.
4. Weigler, H.; Fischer, R.: Influence of high temperatures on strength and deformations of concrete. ACI Seminar on 'Concrete for Nuclear Reactors'. (C. E. Kesler, Ed.), ACI SP 34-26, Berlin, pp. 481-493, 1972.
5. Ehm, C.: Versuche zur Festigkeit und Verformung von Beton unter zweiaxialer Beanspruchung und hohen Temperaturen. Dissertation Technical University Braunschweig, 1986.
6. Jumppanen, U.-M.; Diederichs, U.; Hinrichsmeyer, K.: Material properties of F-concrete at high temperatures. Technical Research Centre of Finland, Research Report No. 452, Espoo, 1986.
7. Thienel, K.-Ch.: Festigkeit und Verformung von Beton bei hoher Temperatur und biaxialer Beanspruchung - Versuche und Modellbildung. Dissertation Technical University Braunschweig, 1993.
8. Thienel, K- Ch.; Rostásy, F.S.: Strength of Concrete Subjected to High Temperature and Biaxial Stress - Experiments and Modeling. Materials and Structures, Vol. 28, pp. 575-581, 1995.
9. Ehm, C.; Kordina, K.; Schneider, U.: The behavior of concrete under biaxial conditions and high temperatures. Int. Conf. on Concrete under Multiaxial Conditions. (RILEM), Vol. II, Presses de l' Université Paul Sabatier, Toulouse, pp. 182-190, 1984.
10. Rostásy, F.S.; Ehm, C.; Hinrichsmeyer, K.: Structural alterations in concrete due to thermal and mechanical stresses. First International Rilem Congress on 'Pore Structure and Materials Properties'. Vol. 1, Paris, 1987.
11. Kordina, K.; Wydra, W.; Ehm, C.: Analysis of the developing damage of concrete due to heating and cooling. ACI Symposium on 'Evaluation of Fire Damage of Concrete and Repair of Damage'. ACI SP 92-6, San Francisco, pp. 87-113, 1986.
12. Thelandersson, S.: On the behavior of concrete exposed to high temperature. Nuclear Engineering and Design, Vol. 75, pp. 271-282, 1983.
13. Thelandersson, S.: Modeling of combined thermal and mechanical action in concrete. Journal of Engineering Mechanics, Vol. 113, No. 6, pp. 893-906, 1987.
14. Stankowski, T.; Gerstle, K.H.: Simple formulation of concrete behavior under multiaxial load histories. ACI Journal, Vol. 82, No. 2, pp. 213-221, 1985.
15. Gerstle, K.H.: Simple formulation of biaxial concrete behavior. ACI Journal, Vol. 78-5, No. 1, pp. 62-68, 1981.
16. Gerstle, K.H.: Simple formulation of triaxial concrete behavior. ACI Journal, Vol. 78-34, No. 5, pp. 382-387, 1981.
17. Thienel, K.-CH.; Rostásy, F.S.: Behaviour of biaxially restrained concrete under high temperature. Transactions of the 12th Int. Conf. on SMiRT. Vol. H, Paper 04/5, Elsevier Science Publishers, Stuttgart, 1993.

Units and Abbreviations

A aggregate content by weight in kg/m^3
C cement content by weight in kg/m^3
E Young's modulus in Gpa
G_{tr} octahedral shear modulus in Gpa
H_{tr} coupling modulus in Gpa

K_{tr} bulk modulus in Gpa
T temperature in °C
W water content by weight in kg/m^3
Y_{tr} coupling modulus in Gpa
f strength in Mpa
$f_{1,20}$ uniaxial compressive strength at normal temperature in Mpa
α stress level, $\alpha = \sigma_{1,20}/f_{1,20}$
γ_{0tr} transient octahedral shear strain in mm/m
ε_{itr} transient principle strain in mm/m, (i = 1, 2, 3)
ε_{0tr} transient octahedral normal strain in mm/m
κ stress ratio, $k = \sigma_{2,20} : \sigma_{1,20}$
σ_i principle stress in MPa, (i = 1, 2, 3)
σ_0 octahedral normal stress in Mpa
τ_0 octahedral shear stress in Mpa
20 value at 20°C